Non-Smooth Dynamics Formulation for Planar Prismatic Joints with Clearances

Ekansh Chaturvedi[1], **Corina Sandu**[2], **Adrian Sandu**[3]

[1] PhD. Student,
Mechanical Engineering Dept.
Virginia Tech
Blacksburg, 24060, USA
ekanshchat96@vt.edu

[2] Professor,
Mechanical Engineering Dept.
Virginia Tech
Blacksburg, 24060, USA
csandu@vt.edu

[3] Professor,
Computer Science Dept.
Virginia Tech
Blacksburg, 24060, USA
sandu@cs.vt.edu

ABSTRACT

Multibody systems can be classified into two categories based on the type of constraints they carry. Ideal constraints in the multibody systems are the ones which enforce absolute alignment of bodies with respect to each other in the desired direction of motion. However, the real-life systems have bodies constrained to each other in joints which have clearances, and the condition of absolute alignment is not followed. The existing multibody formulations deal with such cases by introducing impulse generating contact detection models based on interpenetration of the bodies, which estimate the contact forces using material properties of the bodies in contact using nonlinear spring-damper elements. The high numerical values of Hertzian contact stiffness result in stiff differential equations. Another approach for solving contact problems is non-smooth method that employs equations of motion as mathematical constraints and minimize the action as per the "least action principle". This work delineates a methodology for formulating and simulating non-smooth planar multibody systems. The methodology is demonstrated through a case study on planar prismatic joints with clearances. The overall formulation of the problem has been discussed with emphasis on formulation of geometric constraints that capture all the possible cases of contact formation. Cases are simulated and observations are discussed.

Keywords: Non-smooth dynamics, Prismatic joints, Planar systems, Joint clearances, Contact detection.

1 INTRODUCTION

Multibody systems simulations may consist of multiple constraints that represent mechanical joints in the form of equations. Such constraints enforce absolute alignment of the connected bodies in the desired direction of relative motion. Hence, such constraint equations represent ideal joints. However, real world mechanical systems have joints with clearances and the condition of absolute alignment is not valid and the motion is governed by intermittent formation of multiple contacts. In this section, the existing literature relevant to contact mechanics and constrained multibody dynamics has been studied. Corral et al. [1] introduced a geometry-based contact model that considers penetration for evaluating displacement and restitution. One interesting feature of this model is that it formulates infinite planes to identify the contact points, however, this model does not integrate well with DAE/ODE formulations for constrained multibody systems.

Dopico et al. [2, 3] and Choi et al. [4] used a similar approach for formulating contact models integrable with index-3 DAEs. However, the approach uses discretized mesh representation

of geometry to identify the contact points and hence the constraint manifold is overloaded with equations corresponding to each node. These methods account for dynamics by forcing penalty factors using augmented Lagrangian method by projection of velocity and acceleration at contact points to solve for static equilibrium.

Using the Hertzian contact model developed by Nikravesh and Lankarani [5], Shen et al. [6] developed formulation for simulating impact dynamics by using dynamic optimization with energy loss being the objective function. It must be mentioned at this point that the contact model in [5] has been the one of the most impactful models and has been implemented in the renowned commercial software packages. However, a major concern that arises with using nonlinear spring-damping combination of contact forces with Hertzian method, is that doing so makes the equations of motion very stiff and it requires very small time-step sizes for integration. Further, this also requires separate detection of individual contact and subsequent evaluation of contact forces. This method makes this approach computationally inefficient, especially when multiple contacts occur intermittently.

Until now, various contact models and their applications have been discussed in this section. However, the work most relevant to the scope of this project can be credited to Sharf and Zhang [7] and [8]. Sharf and Zhang in [7] founded the geometry based contact models. Zakhariev in [8] described an approach for calculating the reaction and friction forces between pairs of bodies in spatial mechanical systems, as well as contact points in joints with clearances. Matrix methods were used to derive the nonlinear kinematic constraint equations, and the external and inertia forces for each configuration of the kinematic chain the contact points and corresponding normal forces are calculated. However, a major drawback that could be observed in [8] is that the equality constraints discussed do not account for all the possible orientations of the contact formation.

Further developments in the domain of clearance joints include the work by Ibrahimi et al [9], Flores and Lankarani [10] and Xiang et al. [11], where they conducted simulations on planar systems formulated as DAEs and contact model referenced from [5]. Sensitivity analysis for planar systems was also included in [9] although the sensitivities were not analyzed in the time domain. Bauchau et al. [12] used unilateral contact conditions to simulate planar and spatial joints by adding additional rotational state variables and using non holonomic inequality constraints with introduction of slack variables.

The recent developments in non-smooth dynamics have demonstrated the efficacy of the methodology through many-body dynamics problems such as simulation of sand particles, stacking of bricks and stacking of multiple balls in a box [13, 14, 15], where the formulation of constraints is straight forward. When implementing this approach to multibody systems, a crucial aspect would be the formulation of constraints. Because of shape and geometry of the components, the constraint formulation should capture the possibilities of multiple contact points at different locations yet retaining the analytical nature of the constraint expression. This requirement would be necessary to build computationally efficient codes in contrast to contact detection algorithms that use finite element discretization schemes of the solid bodies.

The discussed literature inspires one to work towards a universal formulation for multibody systems that can simulate systems with ideal constraints, constraints with clearances as well as impact dynamics. The results can be impactful in rationalizing the design procedures as tolerance assignment is a critical task on engineering drawings. Understanding the effect of tolerances on the system's dynamic response can be helpful in optimizing the design of a machine's components.

2 METHODOLOGY

2.1 Formulation of problem

Consider a system of N bodies, of mass m_j and inertia J_j with generalized coordinates designated by $\mathbf{q}_j = [\mathbf{r}^{\mathbf{T}}{}_j, \theta_j]^T \in \mathbb{R}^3$ as a planar system, such that $j \in \mathbb{I}^N$, where the j^{th} particle has mass m_j and inertia J_j. Haug [16] derived the equations of motion for unconstrained systems by leveraging D'Alembert's principle of virtual work:

$$\delta\mathbf{q}\left(\mathbf{M}\left(\mathbf{q}\right)\ddot{\mathbf{q}} + \mathbf{S}\left(\mathbf{q},\dot{\mathbf{q}}\right) - \mathbf{Q_A}\right) = 0 \tag{1}$$

Here, $\mathbf{M}(\mathbf{q})$ is the $3N \times 3N$ combined mass matrix of N bodies. The $3N \times 1$ vector $\mathbf{S}(\mathbf{q},\dot{\mathbf{q}})$ represents the Coriolis force and the $3N \times 1$ vector $\mathbf{Q_A}$ represents external forces and torque acting on the body neglecting friction. Unless the contact happens, the bodies move as an unconstrained system in the free space, following the equation (2):

$$\ddot{\mathbf{q}}_{uc} = -\mathbf{M}\left(\mathbf{q}\right)^{-1}\left(\mathbf{S}\left(\mathbf{q},\dot{\mathbf{q}}\right) - \mathbf{Q_A}\right) \tag{2}$$

Let the gap function Φ^{ineq} be such that $\Phi^{ineq} \leq 0$. If the contact is formed, the work done by constraint reaction forces corresponding to inequality constraints, is 0. Therefore, $\delta\mathbf{q}(\Phi^{ineq}_{\mathbf{q}}(\mathbf{q})) = 0$, where $\Phi^{ineq}_{\mathbf{q}}(\mathbf{q})$ is the Jacobian matrix of the gap function. Using the Lagrangian multipliers [17, 18], the equation of motion transforms to equation (3).

$$\mathbf{M}\left(\mathbf{q}\right)\ddot{\mathbf{q}} + \Phi^{ineq^T}_{\mathbf{q}}\left(\mathbf{q}\right)\mu + \mathbf{S}\left(\mathbf{q},\dot{\mathbf{q}}\right) - \mathbf{Q_A} = 0 \tag{3}$$

Where μ is the vector of Lagrange multipliers for each constraint equation. The entity $\Phi^{ineq}(\mathbf{q})* \mu$ represents the element wise product of expressions in the constraint manifold, and the corresponding Lagrange multiplier μ. Therefore:

$$\Phi^{ineq}_{\mathbf{q}}\left(\mathbf{q}\right) * \mu = 0; \mu \geq 0 \tag{4}$$

This equation indicates a complementary condition which basically means if $\Phi^{ineq}(\mathbf{q}) = 0$, $\mu \neq 0$ and if $\mu = 0$, $\Phi^{ineq}(\mathbf{q}) \neq 0$. The physical meaning of this equation is that if the contact happens, i.e., $\Phi^{ineq}(\mathbf{q}) = 0$, μ should not be 0 as it will give out contact forces at each of the contact points. Similarly, if $\Phi^{ineq}(\mathbf{q}) < 0$, it means that the contact has not yet formed and corresponding $\mu = 0$. Furthermore, Gauss' principle of least constraint [19] is a least squares principle stating that the true accelerations of a mechanical system of N masses is the minimum of the quantity:

$$\mathbf{Z} = \sum_{j=1}^{N} m_j \|\ddot{\mathbf{r}} - \frac{\mathbf{F_j}}{m_j}\|^2 \tag{5}$$

where the j^{th} particle has mass m_j, position vector $\mathbf{r}_j$, and applied non-constraint force $\mathbf{F}_j$ acting on the mass. Assuming a constant mass matrix $\mathbf{M} = diag[m_1, m_1, J_1, ..., m_N, m_N, J_N]$ and plugging equations (2) and (3) in equation (5), the governing objective function for the system can be represented as the minimum of the difference in constrained and unconstrained accelerations as shown in equations (6) and (7) .

$$\mathbf{Z} = \left(\ddot{\mathbf{q}} - \ddot{\mathbf{q}}_{uc}\right)^T \mathbf{M}\left(\ddot{\mathbf{q}} - \ddot{\mathbf{q}}_{uc}\right) \tag{6}$$

$$\mathbf{Z} = \left(\mathbf{M}^{-1}\Phi^{ineq^T}_{\mathbf{q}}\left(\mathbf{q}\right)\mu\right)^T \mathbf{M}\left(\mathbf{M}^{-1}\Phi^{ineq^T}_{\mathbf{q}}\left(\mathbf{q}\right)\mu\right) \tag{7}$$

Hence, the problem can be stated as a quadratic programming problem subjected to the comple-

mentary constraints with an objective function to be minimized as given below:

$$\begin{aligned} \min \quad & \left(\mathbf{M}^{-1}\Phi_{\mathbf{q}}^{ineq^T}(\mathbf{q})\,\mu\right)^T \mathbf{M}\left(\mathbf{M}^{-1}\Phi_{\mathbf{q}}^{ineq^T}(\mathbf{q})\,\mu\right) \\ \text{s.t.} \quad & \mathbf{M}\ddot{\mathbf{q}} + \Phi_{\mathbf{q}}^{ineq^T}(\mathbf{q})\,\mu + \mathbf{S}(\mathbf{q},\dot{\mathbf{q}}) - \mathbf{Q_A} = 0 \\ & \Phi^{ineq}(\mathbf{q}) * \mu = 0 \\ & \Phi^{ineq}(\mathbf{q}) \leq 0 \\ & \mu \geq 0 \end{aligned} \tag{8}$$

2.2 Discretization and solution strategy

Available are the accelerations, velocities and positions of the generalized coordinates: $\ddot{\mathbf{q}}_{n-1}$, $\dot{\mathbf{q}}_{n-1}$ and $\mathbf{q}_{n-1}$ respectively at time t_{n-1}. Required is to evaluate the accelerations, velocities and positions of generalized coordinates: $\ddot{\mathbf{q}}_n$, $\dot{\mathbf{q}}_n$ and $\mathbf{q}_n$ respectively at time t_n, with time step h_n. Using implicit Euler's expansion we have the following relationships:

$$\dot{\mathbf{q}}_n = \dot{\mathbf{q}}_{n-1} + h_n\ddot{\mathbf{q}}_n \tag{9}$$

$$\ddot{\mathbf{q}}_n = \frac{\dot{\mathbf{q}}_n - \dot{\mathbf{q}}_{n-1}}{h_n} \tag{10}$$

$$\mathbf{q}_n = \mathbf{q}_{n-1} + h_n\dot{\mathbf{q}}_n \tag{11}$$

$$t_n = t_{n-1} + h_n \tag{12}$$

The optimization problem, as stated in equation (7), at time t_n is formulated as follows:

$$\begin{aligned} \min \quad & \left(\mathbf{M}^{-1}\Phi_{\mathbf{q}}^{ineq^T}(\mathbf{q}_n)\,\mu_n\right)^T \mathbf{M}\left(\mathbf{M}^{-1}\Phi_{\mathbf{q}}^{ineq^T}(\mathbf{q}_n)\,\mu_n\right) \\ \text{s.t.} \quad & \mathbf{M}\ddot{\mathbf{q}}_n + \Phi_{\mathbf{q}}^{ineq^T}(\mathbf{q}_n)\,\mu_n + \mathbf{S}(\mathbf{q}_n,\dot{\mathbf{q}}_n) - \mathbf{Q_A} = 0 \\ & \Phi^{ineq}(\mathbf{q}_n) * \mu_n = 0 \\ & \Phi^{ineq}(\mathbf{q}_n) \leq 0 \\ & \mu_n \geq 0 \end{aligned} \tag{13}$$

Plugging the expressions from equations (10-12), we get the following optimization problem at the time t_n:

$$\begin{aligned} \min \quad & \left(\mathbf{M}^{-1}\Phi_{\mathbf{q}}^{ineq^T}(\mathbf{q}_{n-1}+h_n\dot{\mathbf{q}}_n)\,\mu_n\right)^T \mathbf{M}\left(\mathbf{M}^{-1}\Phi_{\mathbf{q}}^{ineq^T}(\mathbf{q}_{n-1}+h_n\dot{\mathbf{q}}_n)\,\mu_n\right) \\ \text{s.t.} \quad & \mathbf{M}\left(\frac{\dot{\mathbf{q}}_n - \dot{\mathbf{q}}_{n-1}}{h_n}\right) + \Phi_{\mathbf{q}}^{ineq^T}(\mathbf{q}_{n-1}+h_n\dot{\mathbf{q}}_n)\,\mu_n + \mathbf{S}(\mathbf{q}_{n-1}+h_n\dot{\mathbf{q}}_n,\dot{\mathbf{q}}_n) - \mathbf{Q_A} = 0 \\ & \Phi^{ineq}(\mathbf{q}_{n-1}+h_n\dot{\mathbf{q}}_n) * \mu_n = 0 \\ & \Phi^{ineq}(\mathbf{q}_{n-1}+h_n\dot{\mathbf{q}}_n) \leq 0 \\ & \mu_n \geq 0 \\ & h_{\varepsilon^+} \geq h_n \geq h_{\varepsilon^-} \end{aligned} \tag{14}$$

Here, the optimal values of h_n, μ_n and $\dot{\mathbf{q}}_n$ need to be found at time t_n. The scalar terms h_{ε^+} and h_{ε^-} respectively, are the minimum and maximum finite positive values of time-step size. Once the optimization problem has been solved at a time t_n, the value of $\dot{\mathbf{q}}_n$ and h_n can then be utilized to evaluate and store the accelerations $\ddot{\mathbf{q}}_n$ and the positions $\mathbf{q}_n$ using equations (10) and (11).

2.3 Formulation of constraints for prismatic joints with clearances

Figure 1 shows a system of two bodies i and j forming a prismatic pair with two-sided clearance c. The generalized coordinates of bodies are $\mathbf{q}_i \in \mathbb{R}^3$ and $\mathbf{q}_j \in \mathbb{R}^3$ respectively. Let points $\mathbf{a}$ and $\mathbf{b}$ represent the two ends of center-line of body j in global frame of reference. Let points $\mathbf{p}$ and $\mathbf{r}$ represent the two ends of center-line of body i in global frame of reference. The perpendicular distances of points $\mathbf{p}$ and $\mathbf{r}$ from the center axis of body j are $\mathbf{d_p}$ and $\mathbf{d_r}$ respectively. Let $\mathbf{A}(\theta_\mathbf{i})$ $\mathbf{A}(\theta_\mathbf{j})$ be the rotation matrices of the respective bodies. Given the local coordinate vector $\mathbf{s'_i}$ of an arbitrary point $\mathbf{x}$ in body i, the position of point $\mathbf{x}$ can be evaluated in global frame as $\mathbf{r_x}$ using equation (15).

$$\mathbf{r_x} = \mathbf{r_i} + \mathbf{A}(\theta_\mathbf{i})\mathbf{s'_i} \tag{15}$$

Figure 2 illustrates the possible cases on contact between the two bodies. Considering c of a very small magnitude in comparison to other dimensions of the components, the perpendicular distances $\mathbf{d_p}$ and $\mathbf{d_r}$ should always be follow the inequalities (16).

$$\begin{bmatrix} \mathbf{d_p} - c \\ \mathbf{d_r} - c \end{bmatrix} \leq 0 \tag{16}$$

The perpendicular distance of a point $\mathbf{k} \in [\mathbf{p}, \mathbf{r}]$ from a line passing through points $\mathbf{a}$ and $\mathbf{b}$ can be evaluated as per equation (17)

.

$$\mathbf{d_k} = \|(\mathbf{k}-\mathbf{a}) - \frac{(\mathbf{k}-\mathbf{a}).(\mathbf{b}-\mathbf{a})}{||\mathbf{b}-\mathbf{a}||}\| \tag{17}$$

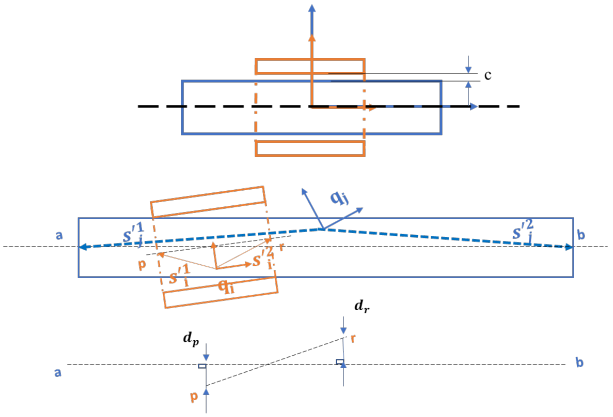

Figure 1: Schematic representation of planar prismatic joint with clearance

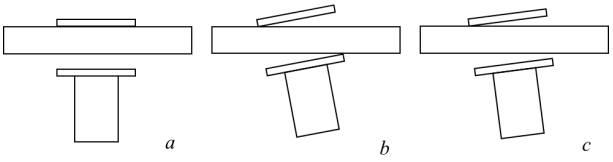

Figure 2: Contact cases: *a*. Line contact, *b*. two-point contact, *c*. single-point contact

Furthermore, the maximum possible angular misalignment can be represented as $\frac{c}{2l}$ where $l = min(|\mathbf{p}-\mathbf{r}|, |\mathbf{a}-\mathbf{b}|)$. The constraint on angular misalignment $\delta\theta$ can be evaluated as the angle between the vectors $\mathbf{d}_i = \mathbf{r} - \mathbf{p}$ and $\mathbf{d}_j = \mathbf{b} - \mathbf{a}$ as per equation (18).

$$\delta\theta = \cos^{-1} \frac{\mathbf{d_i}.\mathbf{d_j}}{||\mathbf{d_i}||.||\mathbf{d_j}||} \tag{18}$$

Hence, the complete constraint vector for a planar prismatic joint with clearance is given in equation (19)

$$\Phi^{prism}(\mathbf{q}_n) = \begin{bmatrix} \mathbf{d_p} - c \\ \mathbf{d_r} - c \\ \delta\theta - \frac{c}{2l} \end{bmatrix} \leq 0 \tag{19}$$

2.4 Algorithm

A step-by-step procedure to implement the formulation discussed in previous section has been explained below. For a target simulation time t_{max}:

1. Start with initial values of $\mathbf{Y_0} = \mathbf{Y_{n-1}} = [h_{n-1}, \mu^{\mathbf{T}}_{\mathbf{n-1}}, \dot{\mathbf{q}}^T_{n-1}]^T$ at time $t_0 = t_{n-1}$ such that constraint equations in (13) are satisfied. For the initial values of generalized coordinates satisfying a negative value of gap function, the initial value of Lagrangian multipliers should be assumed zero.

2. Perform optimization as per equation (14) with $\mathbf{Y_0} = \mathbf{Y_{n-1}}$ as initial guess solution. Optimization toolbox of the numerical analyses software prove to be very effective. Recommended optimization algorithms include sequential quadratic programming and interior point methods.

3. Obtain the optimal values of $\mathbf{Y_n} = [h_n, \mu^{\mathbf{T}}_{\mathbf{n}}, \dot{\mathbf{q}}^T_n]^T$ and evaluate time, positions, and accelerations as per equations (10-12).

4. Store the values of t_n, $\mathbf{q}_n$, $\dot{\mathbf{q}}_n$ and $\ddot{\mathbf{q}}_n$ in the corresponding vectors and assign $\mathbf{Y_{n-1}} = \mathbf{Y_n}$.

5. Repeat the steps 2, 3, and 4 until $t_n = t_{max}$.

3 CASE STUDY

Figure 3 shows a simple case study of a planar prismatic joint with clearance to illustrate the proof of concept for the proposed formulation. The case study comprises of a slider of mass m and rotational inertia J with its center of mass denoted by the generalized coordinates $\mathbf{q} \in \mathbb{R}^3$ and a mass-less rod fixed at both ends. There is a clearance $c = 10\mu m$ between the slider and the rod and gravity acts along the $-\mathbf{Y}$ axis. An external force $\mathbf{F} = [f_x, f_y, \tau_\theta]^T \in \mathbb{R}^3$ acts on the slider at a point marked by a body-frame vector $\mathbf{s}'_f$.

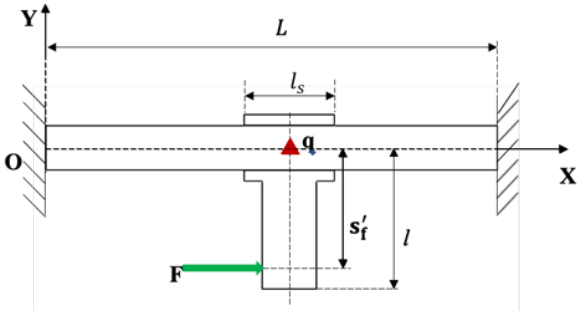

Figure 3: Schematic diagram of the case study

Keeping the inertial properties and applied external force constant, the following three cases are possible depending on the length of $\mathbf{s}'_f$ denoted by $|\mathbf{s}'_f|$:

1. If $|\mathbf{s}'_f|$=0, i.e., the force f_x acts on the center of mass $\mathbf{q}$, and gravity acting along the -Y axis.

2. If $|\mathbf{s'}_f|$ is a small value relative to the full length of the protrusion l, the torque applied by gravity, acting along the -Y axis, about any contact point could surpass the torque generated by the applied force f_x.

3. If $|\mathbf{s'}_f| = l$ with no gravity.

The system specific details illustrated in Figure 3 are shown in Table 1.

Table 1: Case study specifications

Property	Value	Units
m	5	kg
J	800	$kg - mm^2$
L	100	mm
l_s	20	mm
l	10	mm
f_x	50	N

4 RESULTS AND DISCUSSION

The simulation results were achieved with time step varying between $1e^{-4}$ and $1e^{-3}$ seconds with constraint violation $||\Phi^{ineq}(\mathrm{q})|| \leq 1e^{-8}$ upon the contact formation. At the same time the equations of motion (3) were satisfied within the limits of $1e^{-12}$.

4.1 Case 1: $|\mathbf{s'}_f| = 0$

As discussed in section 3, if $|\mathbf{s'}_f| = 0$, there is no external torque acting on the slider. As expected, in the absence of the applied external torque, the slider would retain its initial angular orientation. However, gravity pulls the slider downwards to make a line contact with the rod. Figure 4 represents the positions of centroid, left end and right end of the slider, against time, in y and x directions respectively. Figure 5 shows the centroidal velocities in y and x directions respectively and Figure 6 shows contact forces acting on slider against time.

4.2 Case 2: $|\mathbf{s'}_f| << l$

For second case, $|\mathbf{s'}_f|$ was taken as 0.5mm. While the X-position and velocities remain unchanged, Figures 7, 8 and 9 represent the Y-positions, velocities and contact forces respectively. It can be observed that the slider retains a single point contact for most of the time at the left end, though intermittently forming contact at the right end as well.

4.3 Case 3: $|\mathbf{s'}_f| = l$

In case 3, the external torques acting on the slider is sufficient enough to make slider contact the rod at two diametrically opposite ends. The slider changes its angular orientation until point contact is detected at each end of the slider. After contact detection, the slider retains its angular orientation and moves along x direction without losing contact. Just as in case 1, the X-direction entities remain unchanged. The figures 10, 11, and 12 represent the Y direction positions, velocities, and contact forces respectively.

5 CONCLUSIONS

The simulation results demonstrate the efficiency of the non-smooth dynamics methodology for simulating the joints with clearance. The mathematical representations of constraint inequalities were carefully derived to ensure that they capture all the possible scenarios of contact formation.

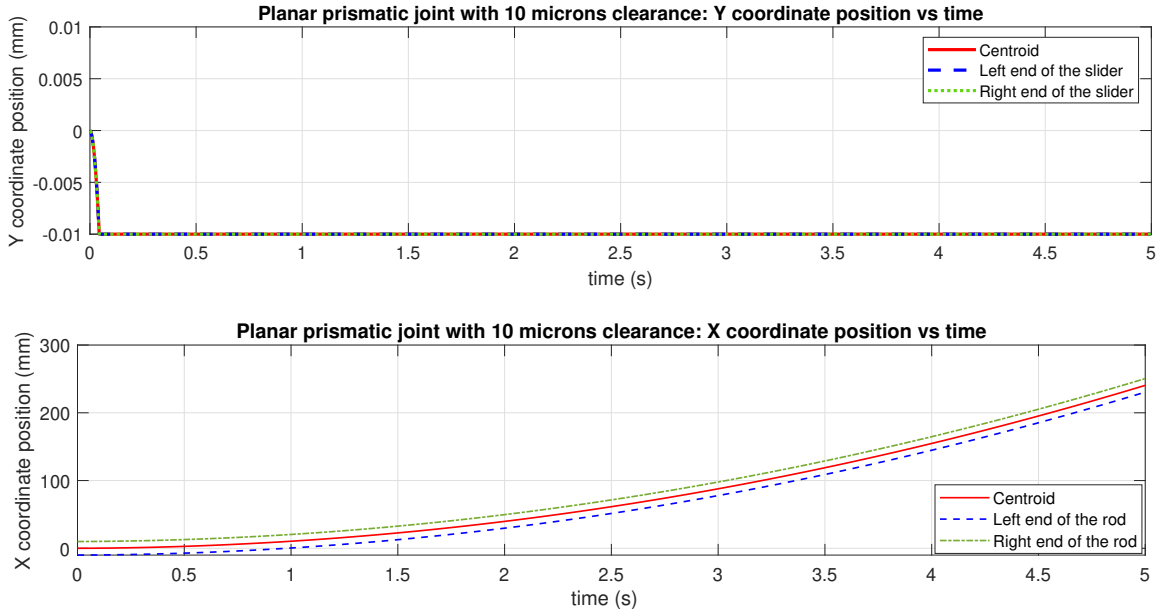

Figure 4: Case 1: Position vs time

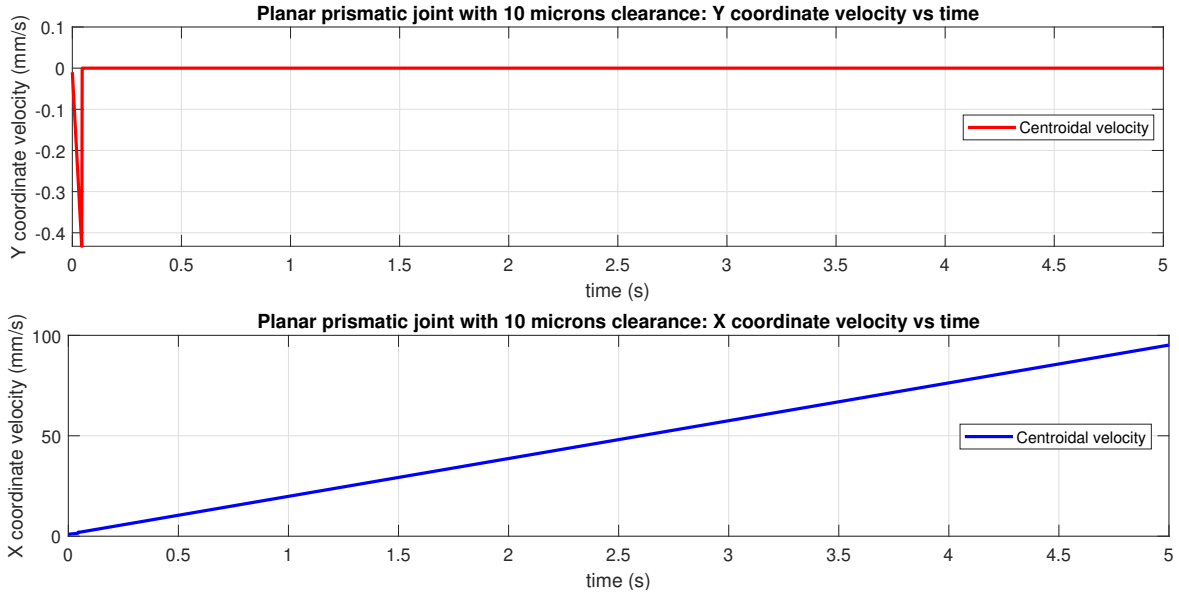

Figure 5: Case 1: Velocity vs time

The results showed that the tolerance limits of constraints during contact are also satisfied within significant accuracy. The computational time for the popular continuous contact models is relatively higher as these models evaluate contact impulse using nonlinear spring-damper elements as functions of interpenetration between the bodies. The resulting high stiffness of the differential equation often requires small time-step sizes during contact force evaluation. This makes the continuous contact models computationally expensive, especially when the contacts break and form intermittently. The computational expense of the presented non-smooth formulation was observed to be low and consistent as the time step size of $1e^{-3}$ was found sufficient for a stable solution.

Though the scope of this work included frictionless contacts, an interesting inference may be drawn from the contact force plots. The magnitude of normal contact force varies significantly

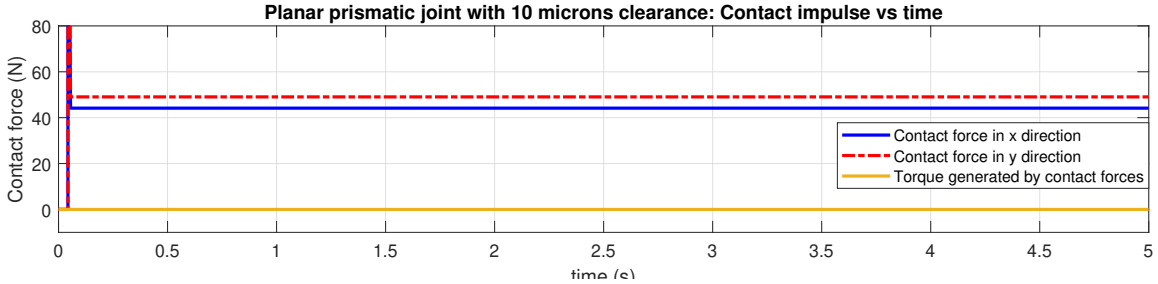

Figure 6: Case 1: Contact forces vs time

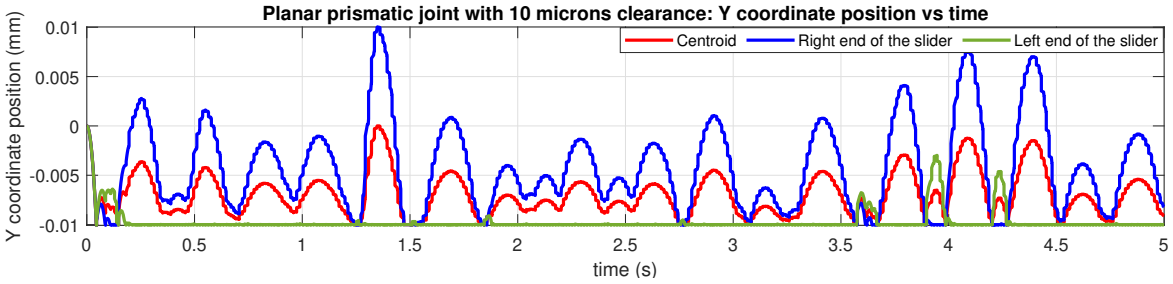

Figure 7: Case 2: Y coordinates vs time

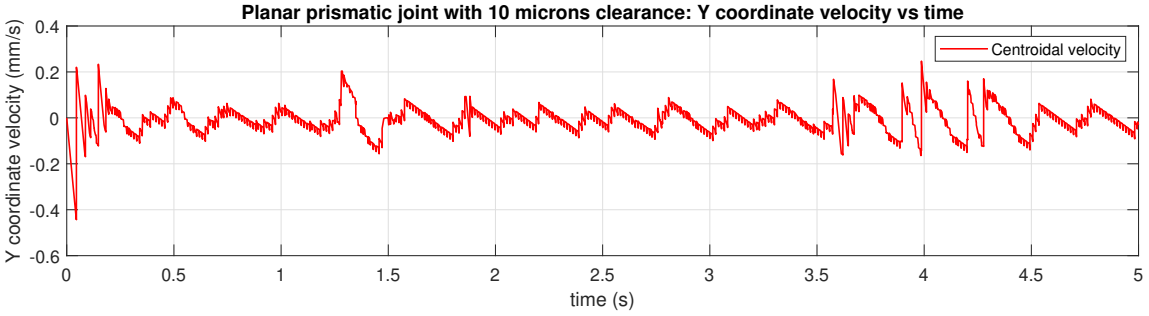

Figure 8: Case 2: Y velocity vs time

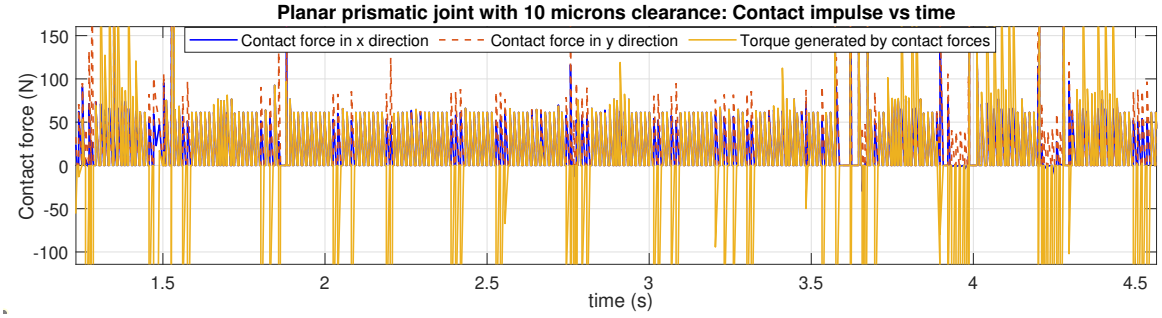

Figure 9: Case 2: Contact forces vs time

among the three cases discussed. Since the resisting friction force depends on the normal contact force's magnitude, adding friction to these simulations will impact the dynamic characteristics to a significant extent. Studying friction in clearance joints will further throw light upon the importance of clearances on the system's dynamics. Besides adding friction, the further scope of this work

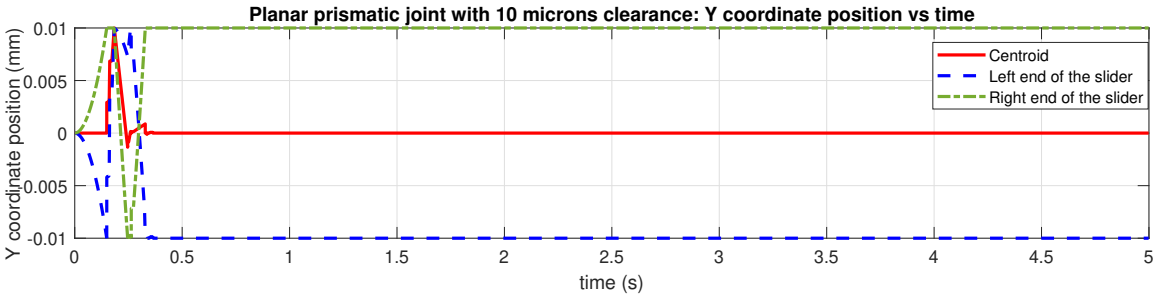

Figure 10: Case 3: Y coordinates vs time

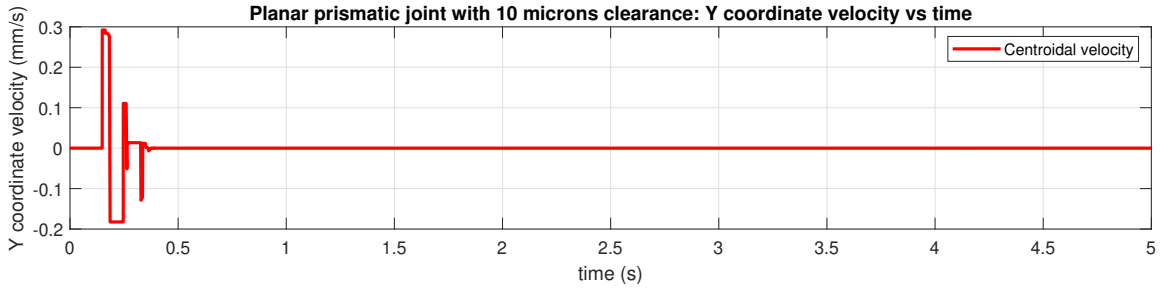

Figure 11: Case 3: Y velocity vs time

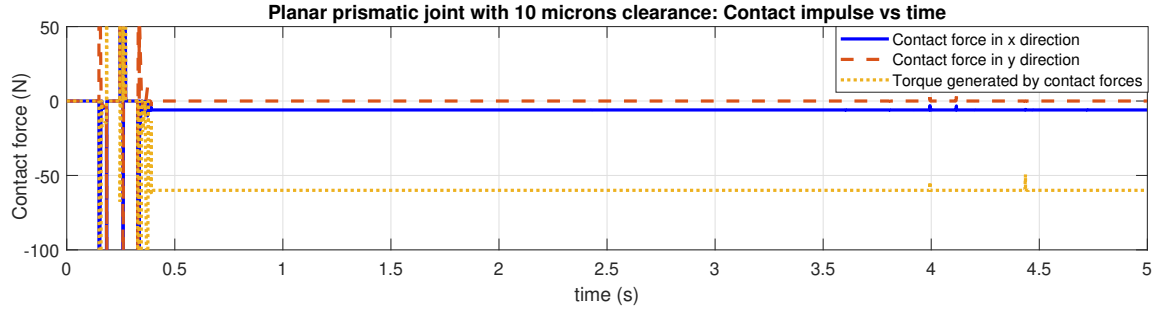

Figure 12: Case 3: Contact forces vs time

includes studying planar revolute joints with clearance and then extending the methodology for spatial systems.

ACKNOWLEDGMENTS

This work was supported by TMVS Lab, Virginia Tech, Blacksburg, USA.

REFERENCES

[1] Corral, E., Moreno, R., Meneses, J., Garcia, M., Castejón, C.: Spatial algorithms for geometric contact detection in multibody system dynamics. Mathematics **9** (2021) 1359 https://doi.org/10.3390/ math9121359.

[2] Dopico, D., Luaces, A., Saura, M., Cuadrado, J., Vilela1, D.: Simulating the anchor lifting maneuver of ships using contact detection techniques and continuous contact force models. Multibody System Dynamics **46** (2019) 147–179

[3] Dopico, D., Gonzalez, F., Cuadrado, J., Kövecses, J.: Determination of holonomic and nonholonomic constraint reactions in an index-3 augmented lagrangian formulation with velocity and acceleration projections. J. Comput. Nonlinear Dynam. **9** (2014) 041006

[4] Choi, J., Ryu, H., Kim, C., Choi, J.: An efficient and robust contact algorithm for a compliant contact force model between bodies of complex geometry. Multibody System Dynamics **23** (2010) 99

[5] Nikravesh, P., Lankarani, H.: A contact force model with hysteresis damping for impact analysis of multibody systems. Journal of Mechanical Design **112** (1990) 369–376

[6] Shen, Y., Xiang, D., Wang, X., Wei, Y.: A contact force model considering constant external forces for impact analysis in multibody dynamics. Multibody System Dynamics **44** (2018) 397–419

[7] Sharf, I., Zhang, Y.: A contact force solution for non-colliding contact dynamics simulation. Multibody System Dynamics **16** (2006) 263–290

[8] Zakhariev, E.: Dynamics of rigid multibody systems with clearances in the joints. Mech. Struct. Mach. **27** (1999) 63–87

[9] Ibrahimi, S., Salahshoor, E., Nouri, S.: Sensitivity analysis for optimal design of multibody systems with clearance joint. Journal of Manufacturing Technology Management **11** (2018) 35–44

[10] Flores, P., Lankarani, H.: Dynamic response of multibody systems with multiple clearance joints. J. Comput. Nonlinear Dynam. **7** (2012) 031003

[11] Xiang, W., Yan, S., Wu, J., Niu, W.: Dynamic response and sensitivity analysis for mechanical systems with clearance joints and parameter uncertainties using chebyshev polynomials method. Mechanical Systems and Signal Processing **138** (2020) 106596

[12] Bauchau, O., Rodriguez, J., Bottasso, C.: Modeling of unilateral contact conditions with application to aerospace systems involving backlash, freeplay and friction. Mechanics Research Communications **28** (2001) 571–599

[13] Jean, M.: The non-smooth contact dynamics method. Computer Methods in Applied Mechanics and Engineering **177** (1999) 235–257

[14] Silcowitz-Hansen, M., Niebe, S., Erleben, K.: A nonsmooth nonlinear conjugate gradient method for interactive contact force problems. Vis. Comput. **26** (2010) 893–901

[15] Anitescu, M.: Optimization-based simulation of non-smooth rigid multibody dynamics. Mathematical Programming **105**(1) (2006) 113–143

[16] Haug, E.: Computer-aided kinematics and dynamics of mechanical systems: basic methods. Allyn and Bacon Series in Engineering (1988)

[17] Anitescu, M., Tasora, A.: An iterative approach for cone complementarity problems for nonsmooth dynamics. Comput. Optim. Appl. **47** (2010) 207–235

[18] Todorov, E.: Convex and analytically-invertible dynamics with contacts and constraints: Theory and implementation in mujoco. In: 2014 IEEE International Conference on Robotics and Automation (ICRA). (2014) 6054–6061 10.1109/ICRA.2014.6907751.

[19] Gauß, C.: Über ein neues allgemeines grundgesetz der mechanik. Zenodo **13** (1829) 1448816 doi:10.1515/crll.1829.4.232.